HHS Public Access

Author manuscript

Aliment Pharmacol Ther. Author manuscript; available in PMC 2018 March 01.

Published in final edited form as:

Aliment Pharmacol Ther. 2017 March ; 45(6): 844–854. doi:10.1111/apt.13951.

Assessment of treatment response in nonalcoholic steatohepatitis using advanced magnetic resonance imaging measures

Steven C. Lin[1,2,*], **Elhamy Heba**[3,*], **Ricki Bettencourt**[2,4], **Grace Y. Lin**[5], **Mark A. Valasek**[5], **Ottar Lunde**[6], **Gavin Hamilton**[3], **Claude B. Sirlin**[3], and **Rohit Loomba**[2,4,7]

[1]Division of Gastroenterology, Beth Israel Deaconess Medical Center, Harvard Medical School, Boston, MA

Contact Information of Corresponding Author: Rohit Loomba, MD, MHSc, Professor of Medicine, Division of Gastroenterology, Director, UCSD NAFLD Research Center, Adjunct Professor, Division of Epidemiology, University of California at San Diego, Biomedical Research Facility II, 4A18, 9500 Gilman Drive, La Jolla, CA 92093, Ph: 858-534-2624, Fax: 858-534-3338, roloomba@ucsd.edu, Website: http://fattyliver.ucsd.edu.

*Co-first Authors

SINC Credit Roster

Members of the San Diego Integrated NAFLD Research Consortium (SINC):
University of California San Diego, La Jolla, CA: Rohit Loomba, MD, MHSc (Principal Investigator of SINC), Ottar Lunde, MD; Heather Hofflich, DO; Yuko Kono, MD; Alexander Kuo, MD; Heather Patton, MD; Michel Mendler, MD; Irine Vodkin, MD; Lisa Richards, NP; Joanie Salotti, NP; Linda Soaft, NP; Barbara Andrews, NP
Sharp Health System, San Diego, CA: Tommy Yen, MD; Michael Bennett, MD; John Person, MD; Cynthia Behling, MD; James Wolosin, MD; Steven Brozinsky, MD
Kaiser Permanente of Southern California, San Diego, CA: Lisa Nyberg, MD; Anders Nyberg, MD; Mamie Dong, MD
Balboa Naval Medical Center, San Diego, CA: Lt. CMDR William Shields, MD, and Len Philo, MD

Writing Assistance: N/A

Conflict of Interest: None disclosed.

Authorship Statement:

i. Guarantor of the article: Rohit Loomba, MD, MHSc

ii. Author contributions and contacts:

- Steven C. Lin (slin6@bidmc.harvard.edu): Drafting of the manuscript, analysis and interpretation of data, critical revision of the manuscript, approved final submission
- Elhamy Heba (elhamyrheba@gmail.com): Drafting of the manuscript, interpretation of data, critical revision of the manuscript, approved final submission
- Ricki Bettencourt (rbettencourt@ucsd.edu): Data analysis, critical revision of the manuscript, approved final submission
- Grace Y. Lin (g4lin@ucsd.edu): Analysis of pathology slides, critical revision of the manuscript, approved final submission
- Mark A. Valasek (mvalasek@ucsd.edu): Analysis of pathology slides, critical revision of the manuscript, approved final submission
- Ottar Lunde (olunde@ucsd.edu): Data analysis, critical revision of the manuscript, approved final submission
- Gavin Hamilton (ghamilton@ucsd.edu): Data analysis, critical revision of the manuscript, approved final submission
- Claude B. Sirlin (csirlin@ucsd.edu): MRI analysis, analysis and interpretation of data, critical revision of the manuscript, obtained funding, study supervision, approved final submission
- Rohit Loomba (roloomba@ucsd.edu): Study concept and design, analysis and interpretation of data, drafting of the manuscript, critical revision of the manuscript, obtained funding, study supervision, approved final submission

iii. All authors approved the final version of this manuscript

[2]NAFLD Research Center, University of California at San Diego, La Jolla, CA

[3]Liver Imaging Group, Department of Radiology, University of California at San Diego, La Jolla, CA

[4]Division of Epidemiology, Department of Family Medicine and Public Health, University of California at San Diego, La Jolla, CA

[5]Department of Pathology, University of California at San Diego, La Jolla, CA

[6]Department of Medicine, University of California at San Diego, La Jolla, CA

[7]Division of Gastroenterology, University of California at San Diego, La Jolla, CA

Abstract

Background—Magnetic resonance imaging derived measures of liver fat and volume are emerging as accurate, non-invasive imaging biomarkers in non-alcoholic steatohepatitis (NASH). Little is known about these measures in relation to histology longitudinally.

Aims—This study examines this relationship between MRI-derived proton-density fat-fraction (PDFF), total liver volume (TLV), total liver fat index (TLFI), vs. histology in a NASH trial.

Methods—This is a secondary analysis of a 24-week randomized, double-blind, placebo-controlled trial of 50 patients with biopsy-proven NASH randomized to oral ezetimibe 10mg daily (n=25) vs. placebo (n=25). Baseline and post-treatment anthropometrics, biochemical profiling, MRI, and biopsies were obtained.

Results—Baseline mean PDFF correlated strongly with TLFI (Spearman's ρ=0.94, n=45, P<0.0001) and had good correlation with TLV (ρ=0.57, n=45, P<0.0001). Mean TLV correlated strongly with TLFI (ρ=0.78, n=45, P<0.0001). After 24 weeks, PDFF remained strongly correlated with TLFI (ρ=0.94, n=45, P<0.0001), maintaining good correlation with TLV (ρ=0.51, n=45, P=0.0004). TLV remained strongly correlated with TLFI (ρ=0.74, n=45, P<0.0001). Patients with Grade 1 vs. 3 steatosis had lower PDFF, TLV, and TLFI (P<0.0001, P=0.0003, P<0.0001, respectively). Regression analysis of changes in MRI-PDFF vs. TLV indicates that 10% reduction in MRI-PDFF predicts 257 mL reduction in TLV.

Conclusions—MRI-PDFF and TLV strongly correlated with TLFI. Decreases in steatosis were associated with an improvement in hepatomegaly. Lower values of these measures reflect lower histologic-steatosis grades. MRI-derived measures of liver fat and volume may be used as dynamic and more responsive imaging biomarkers in a NASH trial than histology. ClinicalTrials.gov number, NCT01766713.

Keywords

nonalcoholic fatty liver disease; hepatic steatosis; liver volume; non-invasive biomarker

INTRODUCTION

Nonalcoholic fatty liver disease is the most common cause of chronic liver disease in the United States (1, 2). Nonalcoholic steatohepatitis (NASH) is the more progressive form of

NAFLD, and can lead to advanced fibrosis, cirrhosis, and hepatocellular carcinoma(3, 4). It is also associated with central obesity, dyslipidemia, insulin resistance, and an increased risk of cardiovascular disease and mortality(1, 5–7). With a predisposition for the elderly, obese, and diabetic(8),(9), the prevalence of NASH continues to increase along with the growth of these populations(10).

Previous studies have relied primarily on histologic endpoints. More recently, advanced imaging modalities such as magnetic resonance spectroscopy, elastography (MRS, MRE) and magnetic resonance imaging proton density fat fraction (MRI proton-density fat fraction) are emerging as new quantitative biomarkers of fat content and fibrosis(11–16). Moreover, new advanced MRI-derived measures of liver fat and volume are being explored for utility in randomized clinical trials(17–19). This is of significance as changes in liver volume may be an important marker of disease progression or regression, as they are associated with metabolic syndrome(20, 21). Strong associations have also been found between liver enlargement and various cardiovascular risk factors(22, 23). However, no studies to date have examined the cross-sectional and longitudinal relationships of these advanced MRI-derived measures versus histologic features.

In this study, we aimed to examine the cross-sectional and longitudinal relationships between MRI proton-density fat fraction, total liver volume (TLV), and total liver fat index (TLFI) in a secondary analysis of NASH randomized clinical trial. We also aim to compare these measures and their changes over time with histologic features. We hypothesize that improvements in advanced MRI-derived measures will reflect both improvements in steatosis and fibrosis.

METHODS

Study Design and Patients

This study is a secondary analysis of a randomized clinical trial of 50 adults with biopsy-proven NASH undergoing treatment with ezetimibe versus placebo. The data obtained for this analysis is from the MOZART (**M**agnetic res**O**nance imaging and elastography in e**Z**etimibe versus placebo for the **A**ssessment of **R**esponse to **T**reatment in NASH) trial, spanning 24 weeks. Details of the original study design and population—including details of baseline and clinical assessments, inclusion and exclusion criteria, and liver biopsy protocols—have been described previously(24). Briefly, MOZART was a randomized, double-blind, placebo-controlled clinical trial designed to assess the efficacy of oral ezetimibe (10mg daily) versus placebo over a 24-week period for the treatment of NASH). Study participants were derived from the San Diego Integrated NAFLD Research Consortium cohort, a city-wide collaboration for the study of NAFLD (led by R.L.). It has been approved by the FDA under an IND, and the UCSD Institutional Review Board approved the protocol, with all patients having signed informed consent. All authors had access to the study data, and reviewed and approved the final manuscript.

Patients underwent baseline history and physicals, clinical and biochemical evaluation at the start of the study, and these were repeated at the end of the study. In addition, baseline magnetic resonance imaging and liver biopsies were also obtained at both the start of the

study (week 0) and the end (week 24). At baseline, mean ± SD interval between the MRI and liver biopsy at baseline was 72.4 ± 96.1 days, and at follow-up was 12.3 ± 10.5 days. Total liver volumes were measured after the study had been completed. Screening processes also included alcohol history assessment through the Alcohol Use Disorder Identification Test (AUDIT) as well as the Skinner Lifetime Drinking questionnaires—both previously validated. Consolidated Standards of Reporting Trials (CONSORT) guidelines were followed; the trial is registered at ClinicalTrials.gov, NCT01766713.

Magnetic Resonance Imaging Protocols

Proton-density fat fraction—The MRI proton-density fat fraction protocol has been previously described and validated as a standardized and objective measure of liver fat content(25, 26), and has been utilized in several NASH trials(13, 14, 24, 27). Patients were scanned in a supine position using a 3T MR scanner (SIGNA Excite HDxt; GE Medical Systems; Milwaukee, WI), with an 8-channel torso-phased array surface coil centered over the liver. Images were obtained once at baseline, and again at post-treatment. Non-contrast axial-magnitude MR images were obtained of the whole liver using a 2-dimensional spoiled gradient-recalled-echo sequence. A low flip-angle (10°) was used at a repetition time of more than 100ms to minimize T1 effects. Six fractional echo magnitude images were obtained at serial opposed-phase and in-phase echo times 1.15, 2.3, 3.45, 4.6, 5.75, and 6.9 ms in a single breathhold (12–24 s). Other imaging parameters included: 8- to 10-mm slice thickness, 14 to 26 slices covering the whole liver, 0-mm slice gaps, 192 × 192 base matrix, 1signal average, and rectangular field of view adjusted to the body habitus and breath-hold capacity.

By using a custom open-source software plug-in for Osirix (Pixmeo Co, Geneva, Switzerland) that corrects for exponential T2* decay and that incorporates a multipeak fat spectral model, MRI proton-density fat fraction parametric maps were reconstructed offline from the source MR images. Circular regions of interest with a 1-cm radius were placed in each of the 4 right liver lobe segments (segments 5– 8) on the proton-density fat fraction maps. proton-density fat fraction values were recorded for each region of interest/segment, and a final right-lobe MRI proton-density fat fraction value for each participant was obtained by averaging the values of the 4 corresponding regions of interest.

Total liver volume measurement—The total liver volume was calculated through a process requiring segmentation image analysis. A radiology research physician (E.H.) utilized the same MR images utilized to derive proton-density fat fraction and segmented the liver contour manually using a custom-built plug-in developed in MATLAB (MathWorks, Natick, MA). Large vessels and structures abutting the liver peripheral and interior (such as the inferior vena cava, main portal vein, and gallbladder) were excluded. Liver volume was calculated after complete segmentation (done cephalad-caudally) by summing the liver surface area at each segmented slice, and then multiplying this sum by individual slice thickness, in milliliters (mL).

Total liver fat index—Total liver fat index (TLFI, units: % mL) takes into consideration the volume of liver from which proton-density fat fraction is derived(17). It is calculated as

the product of liver volume and the liver mean proton-density fat fraction across all liver segments.

$$\mathrm{TLFI}=(\mathrm{Liver\ Volume})\frac{\sum_{i=1}^{n}(PDFF_i)}{n}$$

Here, *n* denotes the total number of voxels in the segmented volume, PDFF*i* is the proton-density fat fraction in the *i*th voxel. This novel imaging biomarker has been described by Tang et al(17). It has been noted that total liver fat index is not an exact measure of mass, but rather an index of hepatic fat burden.

Statistical analysis

The two-tailed t-test was used for comparison of means for continuous variables across various groups in the study (paired within the ezetimibe and placebo arms, unpaired across the treatment arms). Linear regression was used to evaluate cross-sectional relationships at baseline and at week 24 between three advanced MRI-derived measures, as well as the longitudinal relationships between the changes from baseline to follow-up. Wilcoxon-Mann-Whitney test was performed on all non-normally distributed continuous variables. The Fisher's exact or chi-square ($\chi 2$) tests were used for comparisons between categorical variables, as appropriate. All statistical analyses were performed using SAS version 9.3 (SAS Inc, Cary, NC) GraphPad Prism version 6.07 for Windows, GraphPad Software, San Diego California USA (www.graphpad.com) software. All p-values ≤0.05 were considered statistically significant.

RESULTS

Baseline demographic, biochemical, histologic, and advanced MRI characteristics

A total of fifty patients (62% female) with biopsy-proven NASH were included in this secondary analysis of the MOZART trial. The baseline demographic, biochemical, histologic, and imaging characteristics are shown in (Table 1). The mean age ± SD was 49 ± 14 years, and the mean BMI ± SD was 33.4 ± 5.1. Fourteen (28%) of the patients had diabetes. Baseline median (interquartile range, IQR) MRI proton-density fat fraction, total liver volume, and total liver fat index in these patients were 16.6% (12.8%), 1768.4 mL (540.7 mL), and 285.3 %mL (346.3 %mL), respectively. The median (IQR) NAFLD Activity Score (NAS) was 5.0 (2.0).

Correlations between advanced MRI-derived measures

At baseline, mean MRI proton-density fat fraction correlated strongly with total liver fat index (Spearman's $\rho = 0.94$, n = 45, P<0.0001) and had good correlation with total liver volume ($\rho = 0.57$, n = 45, P<0.0001). Mean total liver volume had strong correlation with total liver fat index ($\rho = 0.78$, n = 45, P<0.0001). These findings remained consistently robust after 24 weeks of treatment (Figure 1). At week 24, mean MRI proton-density fat fraction remained strongly correlated with total liver fat index ($\rho = 0.94$, n = 45, P<0.0001), and maintained good correlation with total liver volume ($\rho = 0.51$, n = 45, P=0.0004).

Additionally, mean total liver volume remained strongly correlated with total liver fat index ($\rho = 0.74$, n = 45, P<0.0001).

MRI-derived measures versus histologic steatosis and fibrosis

Steatosis—At baseline, patients with Grade 1 steatosis (n=14) on histology had a median proton-density fat fraction (%) of 9.0 (3.3), versus 13.5 (6.8) and 22.4 (10.0) in those with Grade 2 (n=13) and Grade 3 steatosis (n=23), respectively (Grade 1 vs. 3, P<0.0001). Median total liver volume (mL) for Grade 1, 2, and 3 steatosis were 1553.0 (363.9), 1646.5 (544.2), and 2081.8 (615.2), respectively (Grade 1 vs. 3, P=0.0003). Median total liver fat index (% mL) for Grade 1, 2, and 3 steatosis were 124.8 (50.9), 206.8 (134.6), and 520.3 (196.2), respectively (Grade 1 vs. 3, P<0.0001). See Figure 2.

At week 24, these trends were similar, though there was no statistically significant difference in total liver volume (% mL) between steatosis grades (Grade 1 vs. 3, P=0.0745). In patients with Grade 1 steatosis (n=14), median proton-density fat fraction (%) was 7.8 (4.4), versus 16.9 (9.0) in Grade 2 steatosis (n=13) and 20.7 (2.7) in Grade 3 steatosis (n=8), respectively (Grade 1 vs. 3, P=0.0011). Median total liver fat index (% mL) in Grade 1, 2, and 3 steatosis was 116.6 (102.4), 412.0 (297.3), and 430.6 (149.1), respectively (Grade 1 vs. 3, P=0.0015).

Fibrosis—At baseline and week 24, median proton-density fat fraction, total liver volume, and total liver fat index were not statistically different between those with without or early/mid-fibrosis (Stage 0–2) versus those with advance fibrosis (Stage 3–4). See Table 2.

MRI-PDFF and TLV by fibrosis stage at baseline and week 24

At baseline, mean MRI proton-density fat fraction remained similar in patients between fibrosis stages 0–2, with a decrease noted between fibrosis stage 2–4. See Figure 3a. This trend was similar at week 24, when mean MRI proton-density fat fraction increased between fibrosis stage 0–2, and then decreased between fibrosis stage 2–4. See Figure 3b. At baseline and week 24, the mean total liver volume trended upwards in patients with fibrosis score of 0–3, and then decreased again in those with fibrosis stage 4.

Longitudinal changes in advanced MRI measures versus changes in histologic steatosis grade

Over 24 weeks, strong correlation was observed between changes in mean liver proton-density fat fraction and changes in total liver volume, in a pooled analysis, with Spearman's $\rho = 0.64$, P<0.0001 (n = 45). See Figure 4. Regression analysis yields the equation $\Delta TLV = 25.7(\Delta MRI\text{-}PDFF) + 50.3$, indicating that a 10% reduction in liver fat by MRI proton-density fat fraction was associated with a 257 mL reduction in total liver volume. No significant correlation was observed between changes in histologic steatosis grade and changes in total liver volume ($\rho = 0.14$, P<0.4185 (n = 35)).

Intra- and inter-reader repeatability of total liver volume

In a secondary analysis of an RCT conducted at our center, the intra-reader repeatability of total liver fat index that incorporates the total liver volume in its assessment was assessed through Bland-Altman analysis, which showed good agreement between readers. The intra-

observer repeatability for reader one and two (in mL) were 56.756.7 ± 183.9; (−127.2, 240.6) and −27.3 ± 110.5; (−137.7, 83.2), respectively. The inter-observer repeatability was 5.1 ± 174.5; (−169.4, 179.6)(17). Further assessment of the intra-reader repeatability of total liver volume in an independent cohort was −3 ± 67 (−70, 64) and 12 ± 97 (−85, 109); inter-reader repeatability was 5 ± 98 (−93, 103)(28). In another cohort, intra-reader repeatability was −19 ± 94 (−113,75) and 30 ± 217 (−187, 247); inter-reader repeatability was 6 ± 123 (−117, 129)(29).”

DISCUSSION

By utilizing a prospective cohort of 50 patients enrolled in a randomized clinical trial with biopsy-proven NASH, this study demonstrates that cross-sectionally at both baseline and week 24, advanced MRI-derived measures of proton-density fat fraction and total liver volume were both strongly correlated with total liver fat index. Proton-density fat fraction also had good correlation with total liver volume. We also show that longitudinally, those with increased proton-density fat fraction also had increased total liver volume. Furthermore, these advanced MRI measures were compared with biopsies. We demonstrate that improvements in MRI-derived measures of liver fat burden and size reflected decreases in histologic steatosis grade at both week 0 and 24.

To our knowledge, this is the first study to assess the relationship of advanced MRI-derived measures of liver fat content and volume to histologic steatosis and fibrosis. The strengths of correlations remained similar between baseline and week 24, indicating longitudinal consistency. However, the varied strengths of correlations between different sets of imaging measures suggest that the use of all three may provide more comprehensive assessment of changes in liver fat burden and size, rather than the use of one measure alone in isolation.

Our findings that median MRI proton-density fat fraction, total liver volume, and total liver fat index reflected Grade 1 histologic-determined steatosis versus Grade 3 suggests that these three measures may have utility in monitoring of treatment response within NASH trials or as surrogates of disease progression or regression. The absence of statistically significant relationships between these advanced MRI measures and histologic fibrosis, however, may be in part limited by the sample size of this analysis, particularly those with stage 3 or 4 fibrosis. Furthermore, this may also be inherent to tissue characteristic of fibrosis, which at different stages may have different phenotypic, or volumetric, variability. We did note a non-statistically significant trend showing a decrease of MRI proton-density fat fraction and total liver volume with advanced (stage 4) fibrosis. Other advanced MR modalities—specifically 2D and 3D MR elastography—appear to have superior sensitivity, specificity, and accuracy for diagnosing and assessing (advanced) fibrosis(15, 30, 31).

Longitudinally, changes in mean MRI proton-density fat fraction over time, but not changes in histologic steatosis grade, correlated significantly with changes in total liver volume. This discrepancy may be explained by several reasons. One, changes in steatosis detected histologically is privy to sampling error, and thus may under-represent the overall degree of steatosis grade change. Furthermore, MRI proton-density fat fraction has been shown to be more sensitive than liver histology for detecting incremental, longitudinal changes in hepatic

fat change(13, 14). Thus, these MRI-derived measures of liver fat and volume appear be more dynamic and responsive than histology.

Context of findings in literature

There is a significant public health burden of patients globally with NAFLD and NASH(1, 2), and the prevalence continues to rise(10). Thus, the number of NASH clinical trials has increased to meet this burden, as have the need for non-invasive diagnostic imaging modalities(32–34). The liver biopsy remains the gold standard for diagnosis, yet it often remains impractical and insufficient due to sampling error and complications, such as bleeding and infections(35, 36). Current ultrasound and computerized tomography (CT) imaging modalities are also limited due to operator dependency, in the obese, and lack sensitivity, specificity and quantification of steatosis(37, 38).

Advanced imaging modalities such as quantitative ultrasound and MRI-derived measures (proton-density fat fraction, total liver volume, total liver fat index) are therefore emerging as accurate, sensitive, and specific imaging biomarkers to assess for fat quantification and fibrosis, transcending the aforementioned shortcomings of conventional ultrasound and CT(15, 25, 39). Given that MR imaging is expensive, this study explores the potential of other measures that can be obtained from a single scan, and the information that can be obtained in lieu of the liver biopsy.

Future studies should incorporate large number of patients and how these MRI measures change in relation to other biomarkers, and metabolic and cardiovascular endpoints(23, 40, 41). Furthermore, total liver fat index will require further validation, though the reference standard for this index is still unknown. Conceptually, this measure better reflects total liver fat burden as it accounts for fat fraction given a certain volume, the latter of which will vary depending on individual height and weight. These studies may also trend individual changes of hepatic steatosis and volume, and investigate what demographic or biochemical characteristics are associated with certain combination/accompanied changes in advanced MRI measures. This may help predict how certain populations or phenotypes respond to future therapeutic interventions for NASH.

Strengths and Limitations

One strength of this analysis is that it utilizes a well-characterized patient population that have biopsy-proven NASH, derived from a randomized, placebo-controlled trial that includes blinding of patients, investigators, radiologists, and pathologists. Furthermore, it utilizes MRI proton-density fat fraction, along with other advanced MRI measures, which has been shown to be more sensitive than biopsy for detecting longitudinal changes(14). Furthermore, we compare the advanced MRI-derived measures directly with histologic features pre and post-treatment with ezetimibe, adding a longitudinal component to our findings. A limitation of this study is that as a pooled analysis, the effect of ezetimibe on our post-treatment MRI measures is uncertain. Furthermore, the small sample size, particularly in the advanced fibrosis subset, may not have provided sufficient power to detect significant changes or correlations in our analysis.

CONCLUSION

In this prospective cohort of patients with biopsy-proven NASH, we demonstrate that advanced MRI-derived measures of proton-density fat fraction, total volume, and total liver fat index correlate well with one another cross-sectionally and longitudinally. These advanced MRI-derived measures also increase and decrease with corresponding grades of histologically determined steatosis. A reduction in liver fat by MRI proton-density fat fraction is associated with improvement in hepatomegaly. These measures may provide additional non-invasive quantitative and qualitative information when utilized in NASH clinical trials, and may be more dynamic and responsive than histology.

Acknowledgments

The authors would like to thank and acknowledge all members of the San Diego Integrated NAFLD Research Consortium (SINC).

Funding Support:

The research reported in this publication was supported by the National Institute of Environmental Health Sciences of the National Institutes of Health (NIH), under award number P42ES010337 (RL). The content is solely the responsibility of the authors and does not necessarily represent the official views of the NIH. This work was also supported by an investigator initiated study grant to Dr. Rohit Loomba (RL) by Merck & co. Inc. The study was conducted at the Clinical and Translational Research Institute, University of California at San Diego. RL is supported in part by the American Gastroenterological Association (AGA) Foundation – Sucampo – ASP Designated Research Award in Geriatric Gastroenterology and by a T. Franklin Williams Scholarship Award; Funding provided by: Atlantic Philanthropies, Inc, the John A. Hartford Foundation, the Association of Specialty Professors, and the American Gastroenterological Association and grant K23-DK090303.

Role of Funding Agencies: Funding agencies did not have any role in the design and conduct of the study, collection, management, analysis or interpretation of the data; preparation, review, or approval of the manuscript. There is no conflict of interest.

Abbreviations

AST	Aspartate Aminotransferase
ALT	Alanine Aminotransferase
BMI	Body Mass Index
HDL	High-Density Lipoprotein
Hgb A1C	hemoglobin A1C
LDL	Low-Density Lipoprotein
Alk Phos	Alkaline Phosphatase
GGT	Gamma- Glutamyl Transferase
MRI-PDFF	magnetic resonance imaging proton-density fat fraction
NAS	NAFLD Activity Score
TLV	total liver volume

TLFI total liver fat index

References

1. Chalasani N, Younossi Z, Lavine JE, Diehl AM, Brunt EM, Cusi K, et al. The diagnosis and management of non-alcoholic fatty liver disease: practice Guideline by the American Association for the Study of Liver Diseases, American College of Gastroenterology, and the American Gastroenterological Association. Hepatology. 2012; 55(6):2005–23. [PubMed: 22488764]
2. Adams LA, Feldstein AE. Non-invasive diagnosis of nonalcoholic fatty liver and nonalcoholic steatohepatitis. Journal of digestive diseases. 2011; 12(1):10–6. [PubMed: 21091933]
3. Adams LA, Lymp JF, St Sauver J, Sanderson SO, Lindor KD, Feldstein A, et al. The natural history of nonalcoholic fatty liver disease: a population-based cohort study. Gastroenterology. 2005; 129(1): 113–21. [PubMed: 16012941]
4. Starley BQ, Calcagno CJ, Harrison SA. Nonalcoholic fatty liver disease and hepatocellular carcinoma: a weighty connection. Hepatology. 2010; 51(5):1820–32. [PubMed: 20432259]
5. Targher G, Day CP, Bonora E. Risk of cardiovascular disease in patients with nonalcoholic fatty liver disease. The New England journal of medicine. 2010; 363(14):1341–50. [PubMed: 20879883]
6. Lincoff AM, Wolski K, Nicholls SJ, Nissen SE. Pioglitazone and risk of cardiovascular events in patients with type 2 diabetes mellitus: a meta-analysis of randomized trials. Jama. 2007; 298(10): 1180–8. [PubMed: 17848652]
7. Younossi Z, Henry L. Contribution of Alcoholic and Nonalcoholic Fatty Liver Disease to the Burden of Liver-Related Morbidity and Mortality. Gastroenterology. 2016; 150(8):1778–85. [PubMed: 26980624]
8. Noureddin M, Yates KP, Vaughn IA, Neuschwander-Tetri BA, Sanyal AJ, McCullough A, et al. Clinical and histological determinants of nonalcoholic steatohepatitis and advanced fibrosis in elderly patients. Hepatology. 2013; 58(5):1644–54. [PubMed: 23686698]
9. Ogden CL, Yanovski SZ, Carroll MD, Flegal KM. The epidemiology of obesity. Gastroenterology. 2007; 132(6):2087–102. [PubMed: 17498505]
10. Williams CD, Stengel J, Asike MI, Torres DM, Shaw J, Contreras M, et al. Prevalence of nonalcoholic fatty liver disease and nonalcoholic steatohepatitis among a largely middle-aged population utilizing ultrasound and liver biopsy: a prospective study. Gastroenterology. 2011; 140(1):124–31. [PubMed: 20858492]
11. Hines CD, Frydrychowicz A, Hamilton G, Tudorascu DL, Vigen KK, Yu H, et al. T(1) independent, T(2) (*) corrected chemical shift based fat-water separation with multi-peak fat spectral modeling is an accurate and precise measure of hepatic steatosis. Journal of magnetic resonance imaging : JMRI. 2011; 33(4):873–81. [PubMed: 21448952]
12. Reeder SB, Cruite I, Hamilton G, Sirlin CB. Quantitative assessment of liver fat with magnetic resonance imaging and spectroscopy. Journal of magnetic resonance imaging : JMRI. 2011; 34(4): 729–49. [PubMed: 21928307]
13. Le TA, Chen J, Changchien C, Peterson MR, Kono Y, Patton H, et al. Effect of colesevelam on liver fat quantified by magnetic resonance in nonalcoholic steatohepatitis: a randomized controlled trial. Hepatology. 2012; 56(3):922–32. [PubMed: 22431131]
14. Noureddin M, Lam J, Peterson MR, Middleton M, Hamilton G, Le TA, et al. Utility of magnetic resonance imaging versus histology for quantifying changes in liver fat in nonalcoholic fatty liver disease trials. Hepatology. 2013; 58(6):1930–40. [PubMed: 23696515]
15. Loomba R, Cui J, Wolfson T, Haufe W, Hooker J, Szeverenyi N, et al. Novel 3D Magnetic Resonance Elastography for the Noninvasive Diagnosis of Advanced Fibrosis in NAFLD: A Prospective Study. The American journal of gastroenterology. 2016
16. Park CC, Nguyen P, Hernandez C, Bettencourt R, Ramirez K, Fortney L, et al. Magnetic Resonance Elastography vs Transient Elastography in Detection of Fibrosis and Noninvasive Measurement of Steatosis in Patients with Biopsy-proven Nonalcoholic Fatty Liver Disease. Gastroenterology. 2016

17. Tang A, Chen J, Le TA, Changchien C, Hamilton G, Middleton MS, et al. Cross-sectional and longitudinal evaluation of liver volume and total liver fat burden in adults with nonalcoholic steatohepatitis. Abdominal imaging. 2015; 40(1):26–37. [PubMed: 25015398]
18. Cui J, Philo L, Nguyen P, Hofflich H, Hernandez C, Bettencourt R, et al. Sitagliptin vs. placebo for nonalcoholic fatty liver disease: A randomized controlled trial. Journal of hepatology. 2016
19. Dulai PS, Sirlin CB, Loomba R. MRI and MRE for non-invasive quantitative assessment of hepatic steatosis and fibrosis in NAFLD and NASH: Clinical trials to clinical practice. Journal of hepatology. 2016; 65(5):1006–16. [PubMed: 27312947]
20. Patel NS, Doycheva I, Peterson MR, Hooker J, Kisselva T, Schnabl B, et al. Effect of weight loss on magnetic resonance imaging estimation of liver fat and volume in patients with nonalcoholic steatohepatitis. Clinical gastroenterology and hepatology : the official clinical practice journal of the American Gastroenterological Association. 2015; 13(3):561–8. e1. [PubMed: 25218667]
21. Giannetti M, Piaggi P, Ceccarini G, Mazzeo S, Querci G, Fierabracci P, et al. Hepatic left lobe volume is a sensitive index of metabolic improvement in obese women after gastric banding. Int J Obes (Lond). 2012; 36(3):336–41. [PubMed: 22143620]
22. Santini F, Giannetti M, Mazzeo S, Fierabracci P, Scartabelli G, Marsili A, et al. Ultrasonographic evaluation of liver volume and the metabolic syndrome in obese women. J Endocrinol Invest. 2007; 30(2):104–10. [PubMed: 17392599]
23. Lin SC, Ang B, Hernandez C, Bettencourt R, Jain R, Salotti J, et al. Cardiovascular risk assessment in the treatment of nonalcoholic steatohepatitis: a secondary analysis of the MOZART trial. Therap Adv Gastroenterol. 2016; 9(2):152–61.
24. Loomba R, Sirlin CB, Ang B, Bettencourt R, Jain R, Salotti J, et al. Ezetimibe for the treatment of nonalcoholic steatohepatitis: assessment by novel magnetic resonance imaging and magnetic resonance elastography in a randomized trial (MOZART trial). Hepatology. 2015; 61(4):1239–50. [PubMed: 25482832]
25. Lin SC, Heba E, Wolfson T, Ang B, Gamst A, Han A, et al. Noninvasive Diagnosis of Nonalcoholic Fatty Liver Disease and Quantification of Liver Fat Using a New Quantitative Ultrasound Technique. Clinical gastroenterology and hepatology : the official clinical practice journal of the American Gastroenterological Association. 2015; 13(7):1337–45. e6. [PubMed: 25478922]
26. Patel NS, Peterson MR, Brenner DA, Heba E, Sirlin C, Loomba R. Association between novel MRI-estimated pancreatic fat and liver histology-determined steatosis and fibrosis in non-alcoholic fatty liver disease. Alimentary pharmacology & therapeutics. 2013; 37(6):630–9. [PubMed: 23383649]
27. Patel NS, Peterson MR, Lin GY, Feldstein A, Schnabl B, Bettencourt R, et al. Insulin Resistance Increases MRI-Estimated Pancreatic Fat in Nonalcoholic Fatty Liver Disease and Normal Controls. Gastroenterology research and practice. 2013; 2013:498296. [PubMed: 24348536]
28. Gotra A, Chartrand G, Massicotte-Tisluck K, Morin-Roy F, Vandenbroucke-Menu F, de Guise JA, et al. Validation of a semiautomated liver segmentation method using CT for accurate volumetry. Acad Radiol. 2015; 22(9):1088–98. [PubMed: 25907454]
29. Gotra A, Chartrand G, Vu KN, Vandenbroucke-Menu F, Massicotte-Tisluck K, de Guise JA, et al. Comparison of MRI- and CT-based semiautomated liver segmentation: a validation study. Abdom Radiol (NY). 2016
30. Loomba R, Schork N, Chen CH, Bettencourt R, Bhatt A, Ang B, et al. Heritability of Hepatic Fibrosis and Steatosis Based on a Prospective Twin Study. Gastroenterology. 2015
31. Loomba R, Wolfson T, Ang B, Hooker J, Behling C, Peterson M, et al. Magnetic resonance elastography predicts advanced fibrosis in patients with nonalcoholic fatty liver disease: a prospective study. Hepatology. 2014; 60(6):1920–8. [PubMed: 25103310]
32. Neuschwander-Tetri BA, Loomba R, Sanyal AJ, Lavine JE, Van Natta ML, Abdelmalek MF, et al. Farnesoid X nuclear receptor ligand obeticholic acid for non-cirrhotic, non-alcoholic steatohepatitis (FLINT): a multicentre, randomised, placebo-controlled trial. Lancet. 2014
33. Noureddin M, Anstee QM, Loomba R. Review: emerging anti-fibrotic therapies in the treatment of non-alcoholic steatohepatitis. Alimentary pharmacology & therapeutics. 2016

34. Arulanandan A, Loomba R. Non-invasive Testing for NASH and NASH with Advanced Fibrosis: Are We There Yet? Curr Hepatol Rep. 2015; 14(2):109–18. [PubMed: 26500833]

35. Schwenzer NF, Springer F, Schraml C, Stefan N, Machann J, Schick F. Non-invasive assessment and quantification of liver steatosis by ultrasound, computed tomography and magnetic resonance. Journal of hepatology. 2009; 51(3):433–45. [PubMed: 19604596]

36. Festi D, Schiumerini R, Marzi L, Di Biase AR, Mandolesi D, Montrone L, et al. Review article: the diagnosis of non-alcoholic fatty liver disease -- availability and accuracy of non-invasive methods. Alimentary pharmacology & therapeutics. 2013; 37(4):392–400. [PubMed: 23278163]

37. Sasso M, Miette V, Sandrin L, Beaugrand M. The controlled attenuation parameter (CAP): a novel tool for the non-invasive evaluation of steatosis using Fibroscan. Clinics and research in hepatology and gastroenterology. 2012; 36(1):13–20. [PubMed: 21920839]

38. Springer F, Machann J, Claussen CD, Schick F, Schwenzer NF. Liver fat content determined by magnetic resonance imaging and spectroscopy. World journal of gastroenterology : WJG. 2010; 16(13):1560–6. [PubMed: 20355234]

39. Permutt Z, Le TA, Peterson MR, Seki E, Brenner DA, Sirlin C, et al. Correlation between liver histology and novel magnetic resonance imaging in adult patients with non-alcoholic fatty liver disease - MRI accurately quantifies hepatic steatosis in NAFLD. Alimentary pharmacology & therapeutics. 2012; 36(1):22–9. [PubMed: 22554256]

40. Arulanandan A, Ang B, Bettencourt R, Hooker J, Behling C, Lin GY, et al. Association Between Quantity of Liver Fat and Cardiovascular Risk in Patients With Nonalcoholic Fatty Liver Disease Independent of Nonalcoholic Steatohepatitis. Clinical gastroenterology and hepatology : the official clinical practice journal of the American Gastroenterological Association. 2015; 13(8): 1513–20. e1. [PubMed: 25661453]

41. Sanyal AJ, Friedman SL, McCullough AJ, Dimick-Santos L. Challenges and opportunities in drug and biomarker development for nonalcoholic steatohepatitis: findings and recommendations from an American Association for the Study of Liver Diseases-U.S. Food and Drug Administration Joint Workshop. Hepatology. 2015; 61(4):1392–405. [PubMed: 25557690]

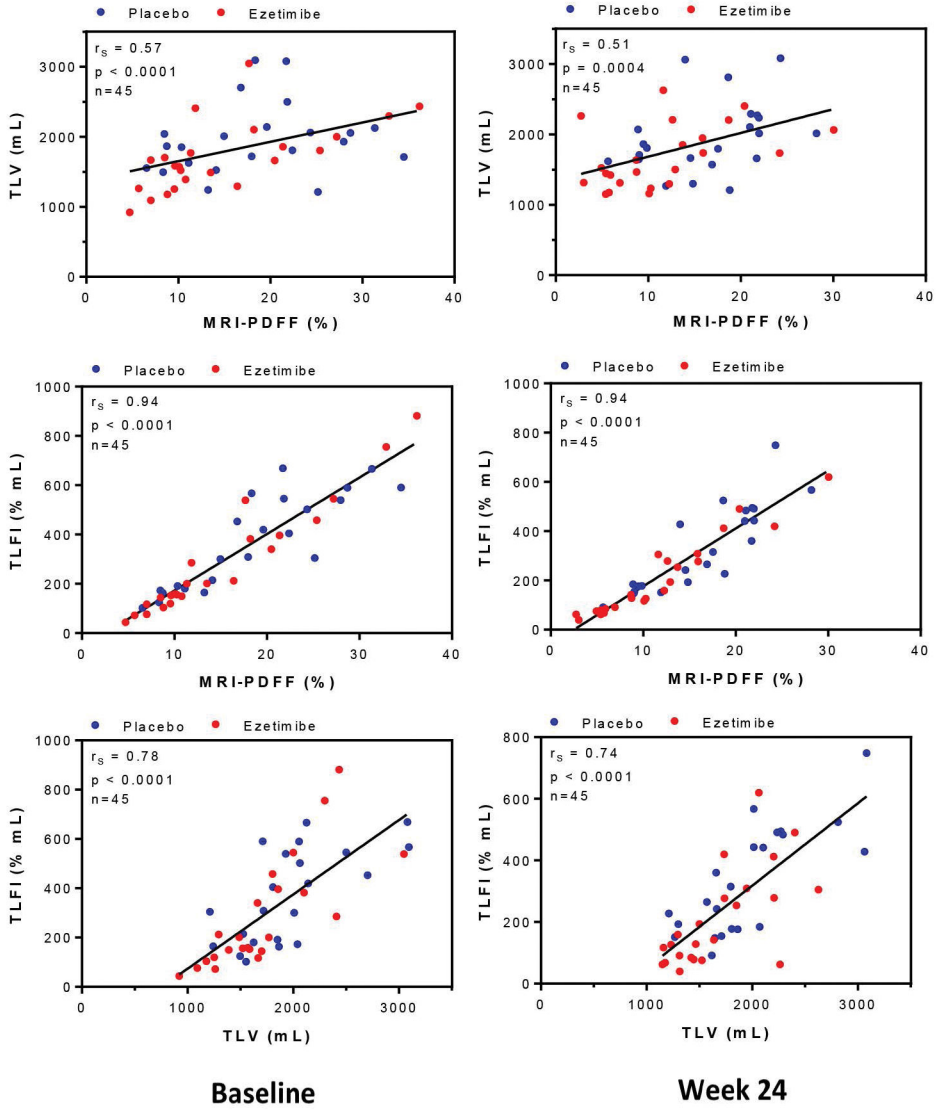

Figure 1. Cross-sectional relationships between advanced MRI-derived measures at baseline and week 24

At baseline, mean PDFF correlated strongly with TLFI (Spearman's ρ = 0.94, n=45, P<0.0001) and had good correlation with TLV (ρ=0.57, n=45, P<0.0001). Mean TLV had strong correlation with TLFI (ρ=0.78, n=45, P<0.0001). These findings remained consistently robust after 24 weeks of treatment. At week 24, mean PDFF remained strongly correlated with TLFI (ρ=0.94, n=45, P<0.0001), and maintained good correlation with TLV (ρ=0.51, n=45, P=0.0004). Additionally, mean TLV remained strongly correlated with TLFI (ρ=0.74, n=45, P<0.0001).

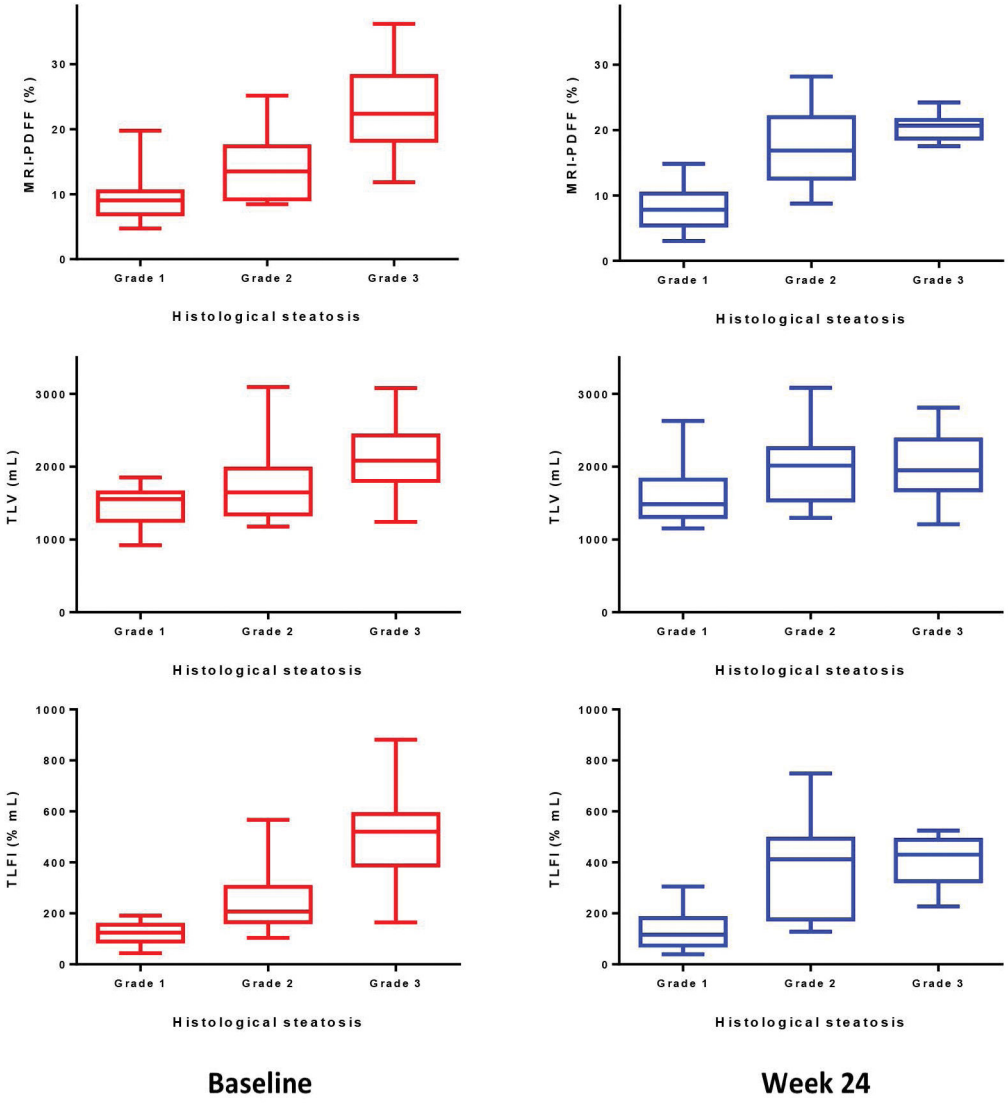

Figure 2. Relationship of advanced MRI-derived measures and histologic steatosis grade at baseline and week 24

At baseline, patients with Grade 1 steatosis (n=14) on histology had a median PDFF (%) of 9.0 (3.3), versus 13.5 (6.8) in Grade 2 steatosis (n=13), and 22.4 (10.0) in those with Grade steatosis (n=23), P<0.0001. Median TLV (mL) for Grade 1, 2, and 3 steatosis were 1553.0 (363.9), 1646.5 (544.2), and 2081.8 (615.2), respectively, P=0.0003. Median TLFI (% mL) for Grade 1, 2, and 3 steatosis were 124.8 (50.9), 206.8 (134.6), and 520.3 (196.2), respectively, P<0.0001. At week 24, median PDFF (%) was 7.8 (4.4) for Grade 1 steatosis (n=14) versus 20.7 (2.7) for Grade 3 steatosis (n=8), P=0.0011. Median TLV (mL) was 1484.2 (494.7) for Grade 1 steatosis versus 1950.1 (650.5) for Grade 3 steatosis, P=0.0745. Median TLFI (% mL) was 116.6 (102.4) for Grade 1 steatosis versus 430.6 (149.1) for Grade 3 steatosis, P=0.0015.

Figure 3a

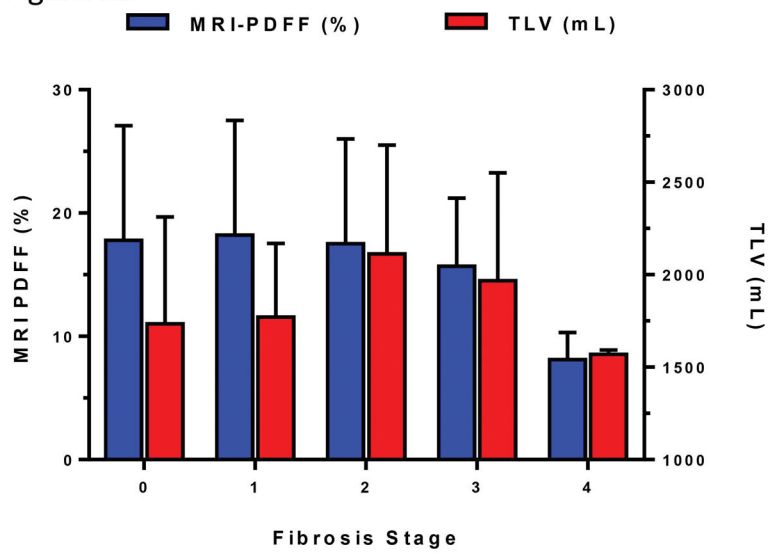

Figure 3b

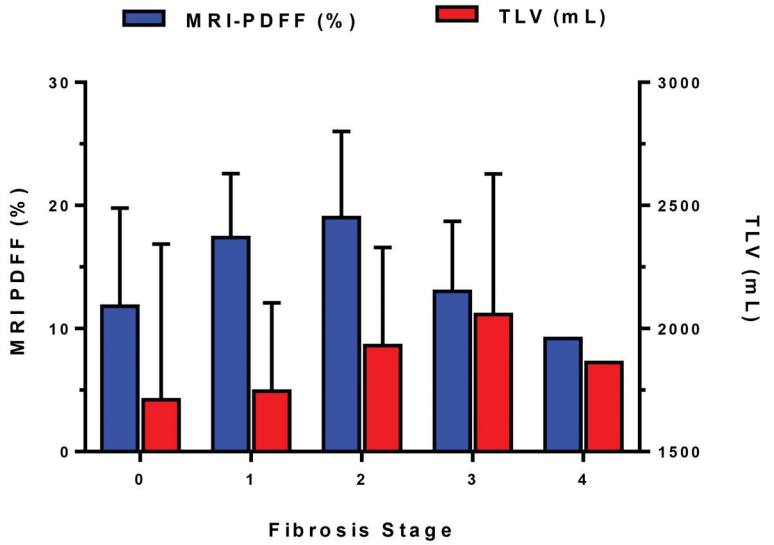

Figure 3. Mean MRI-PDFF and TLV by fibrosis stage at baseline and week 24

(a) At baseline, mean MRI-PDFF % (±SD) with fibrosis stage 0, 1, 2, 3, 4 were 17.8 (9.3), 18.2 (9.3), 17.5 (8.5), 15.7 (5.5), and 8.1 (2.2), respectively. Mean TLV mL (±SD) were 1733.9 (579.0), 1770.5 (398.9), 2112.4 (588.5), 1967.9 (583.7), and 1569.2 (23.0), respectively. (b) At week 24, the trend was similar. Mean MRI-PDFF (%) with fibrosis stage 0, 1, 2, 3, 4 were 11.8 (8.0), 17.4 (5.2), 19.0 (7.0), 13.0 (5.7), 9.2 (0.0), respectively. Mean TLV (mL) were 1710.8 (632.9), 1745.7 (359.1), 1930.8 (399.1), 2057.4 (570.2), and 1862.2 (0.0), respectively.

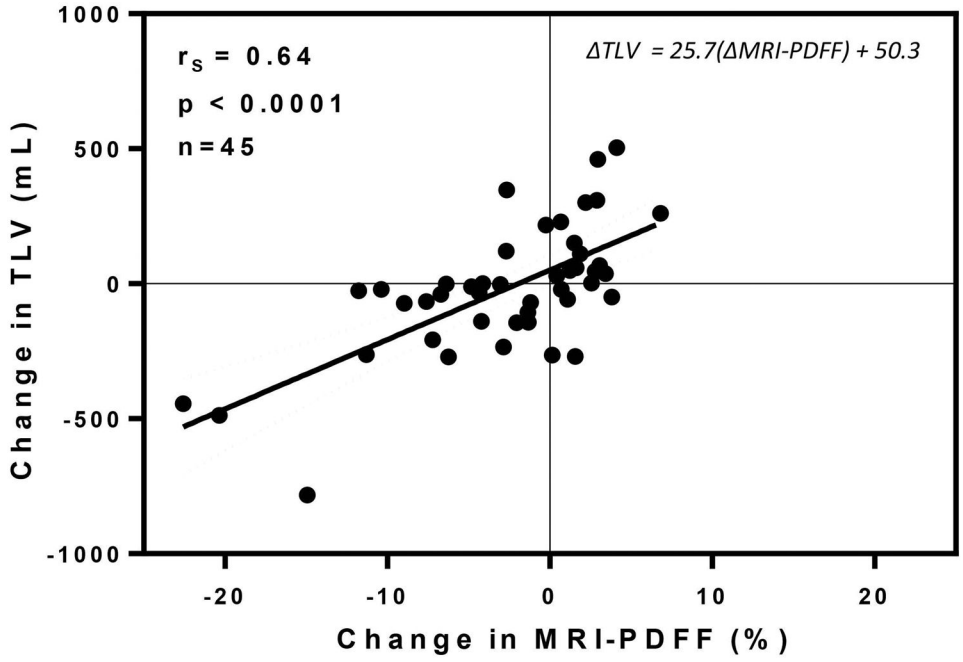

Figure 4. Longitudinal changes in TLV versus MRI-PDFF

Over 24 weeks, strong correlation was observed between changes in MRI-PDFF vs. changes in TLV, in a pooled analysis, with Spearman's ρ=0.64, P<0.0001 (n=45). Regression analysis yields the equation *ΔTLV = 25.7(ΔMRI-PDFF) + 50.3*.

Table 1

Demographic, biochemical and histology characteristics of participants.

	Baseline (n = 50)	Week 24 (n =45)
Demographics		
Female participants	31 (62%)	29 (64%)
Age (years)	49.3 ± 14.2	
Waist (cm)	106.4 ± 11.3	107.4 ± 12.2
Hip (cm)	111.7 ± 9.1	113.7 ± 10.1
Height (m)	1.7 ± 0.1	1.7 ± 0.1
Weight (kg)	93.0 ± 18.3	92.4 ± 19.1
BMI (kg/m2)	33.4 ± 5.1	33.5 ± 5.3
Race and Ethnicity		
White (vs. non-White)	40 (82%)	36 (82%)
Hispanic (vs. non-Hispanic)	17 (34%)	16 (36%)
Diabetes	14 (28%)	14 (31%)
Biochemical profile		
AST (IU/L)	32.5 (28.0)	32.0 (31.0)
ALT (IU/L)	47.5 (30.0)	43.0 (34.0)
Alk Phos	72.0 (31.0)	73.0 (44.0)
GGT (U/L)	40.0 (37.0)	40.5 (31.5)
Total bilirubin (mg/dL)	0.5 (0.3)	0.4 (0.2)
Direct bilirubin (mg/dL)	0.1 (0.1)	0.1 (0.1)
Albumin (g/dL)	4.5 (0.4)	4.5 (0.3)
Glucose (mg/dL)	104.5 (40.0)	102.0 (21.0)
HgA1c (%)	5.9 (0.9)	6.0 (0.8)
Insulin	24.0 (19.0)	29.0 (19.0)
Total cholesterol (mg/dL)	180.5 (38.0)	166.0 (48.5)
Triglycerides (mg/dL)	150.5 (77.0)	130.5 (68.5)
HDL (mg/dL)	44.5 (17.0)	48.5 (17.0)
LDL (mg/dL)	94.0 (38.0)	80.0 (33.0)
Histology		
Steatosis		
1	14 (28.0%)	14 (40.0%)
2	13 (26.0%)	13 (37.1%)
3	23 (46.0%)	8 (22.9%)
Median (IQR)	2.0 (2.0)	2.0 (1.0)
Lobular inflammation		
1	21 (42.0%)	14 (40.0%)
2	29 (58.0%)	20 (57.1%)
3	--	1 (2.9)

	Baseline (n = 50)	Week 24 (n =45)
Median (IQR)	2.0 (1.0)	2.0 (1.0)
Ballooning		
0	4 (8.0%)	6 (17.1%)
1	29 (58.0%)	19 (4.3%)
2	17 (34.0%)	10 (28.6%)
Median (IQR)	1.0 (1.0)	1.0 (1.0)
Fibrosis		
0	15 (30.0%)	11 (31.4%)
1	16 (32.0%)	9 (25.7%)
2	7 (14.0%)	4 (11.4%)
3	10 (20.0%)	10 (28.6%)
4	2 (4.0%)	1 (2.9%)
Median (IQR)	1.0 (2.0)	1.0 (3.0)
NAS		
2	--	4 (11.4%)
3	4 (8.0%)	3 (8.6%)
4	14 (28.0%)	9 (25.7%)
5	14 (28.0%)	9 (25.7%)
6	11 (22.0%)	9 (25.7%)
7	7 (14.0%)	1 (2.9%)
Median (IQR)	5.0 (2.0)	5.0 (2.0)
Imaging		
MRI-PDFF (%)	16.6 (12.8)	12.9 (9.9)
TLV (mL) (N=45)	1768.4 (540.7)	1733.6 (657.9)
TLFI (% mL) (N=45)	285.3 (346.3)	227.5 (291.6)
MRI-PDFF (%)	17.1 ± 8.4	13.9 ± 6.9
TLV (mL) (N=45)	1836.0 ± 514.9	1815.7 ± 493.9
TLFI (% mL) (N=45)	325.9 ± 210.9	268.9 ± 176.1

Mean ± standard deviations presented above for normally distributed variables, median (interquartile range) for non-normally distributed variables. N (%) for categorical variables.

Abbreviations: AST, Aspartate Aminotransferase; ALT, Alanine Aminotransferase; BMI, Body Mass Index; CACs, coronary artery calcium score; FRS, Framingham risk score; HDL, High-Density Lipoprotein; Hgb A1C, hemoglobin A1C; LDL, Low-Density Lipoprotein; Alk Phos, Alkaline Phosphatase; GGT, Gamma- Glutamyl Transferase; MRI-PDFF, magnetic resonance imaging proton-derived fat fraction; NAS, NAFLD Activity Score; TLV, total liver volume; TLFI, total liver fat index.

Table 2a

Advanced MRI-derived measures by steatosis grade at baseline and week 24 – median (IQR)

MRI measure	Histology Determined Steatosis Grade			
	Steatosis 1	**Steatosis 2**	**Steatosis 3**	**P-Value**
Baseline	N = 14	N = 13	N = 23	
PDFF (%)	9.0 (3.3)	13.5 (6.8)	22.4 (10.0)	**<.0001**
TLV (mL)	1553.0 (363.9)	1646.5 (544.2)	2081.8 (615.2)	**0.0003**
TLFI (% mL)	124.8 (50.9)	206.8 (134.6)	520.3 (196.2)	**<.0001**
Week 24	N = 14	N = 13	N = 8	
PDFF (%)	7.8 (4.4)	16.9 (9.0)	20.7 (2.7)	**0.0011**
TLV (mL)	1484.2 (494.7)	2012.9 (664.6)	1950.1 (650.5)	0.0745
TLFI (% mL)	116.6 (102.4)	412.0 (297.3)	430.6 (149.1)	**0.0015**

Abbreviations: MRI, magnetic resonance imaging; PDFF, proton-derived fat fraction; TLV, total liver volume; TLFI, total liver fat index.

Wilcoxon between steatosis grade 1 and grade 3, performed on all continuous/ordinal variables.

Table 2b

Median advanced MRI measures and steatosis grade by fibrosis stage at baseline and week 24

Fibrosis Stage	Baseline					Week 24				
	N	PDFF	TLV	TLFI	Median Steatosis Grade	N	PDFF	TLV	TLFI	Median Steatosis Grade
0–2	38	17.0	1788.3	292.8	2.0	24	14.3	1695.4	240.7	2.0
3–4	12	15.4	1718.2	214.8	2.0	11	12.6	1862.2	265.2	2.0
P-Value		0.2760	0.8234	0.4877	0.4522		0.3019	0.1593	0.9297	0.6243

Abbreviations: MRI, magnetic resonance imaging; PDFF, proton-derived fat fraction; TLV, total liver volume; TLFI, total liver fat index.

Note: Fibrosis stage determined by liver biopsy. P-values from Wilcoxon test F0–2 versus F3–4